

Two novel blue pigments with ellagitannin moiety, rosacyanins A1 and A2, isolated from the petals of *Rosa hybrida*

Yuko Fukui,^{a,*} Kyosuke Nomoto,^{b,*} Takashi Iwashita,^c Katsuyoshi Masuda,^c Yoshikazu Tanaka^d and Takaaki Kusumi^d

^aInstitute for Health Care Science, Suntory Ltd, 1-1-1 Wakayamadai, Shimamoto, Mishima, Osaka 618-8503, Japan

^bFaculty of Life Sciences, Toyo University, 1-1-1 Izumino, Itakura, Gumma 374-0193, Japan

^cSuntory Institute for Bioorganic Research, 1-1-1 Wakayamadai, Shimamoto, Mishima, Osaka 618-8503, Japan

^dInstitute for Advanced Technology, Suntory Ltd, 1-1-1 Wakayamadai, Shimamoto, Mishima, Osaka 618-8503, Japan

Received 23 May 2006; accepted 25 July 2006

Available online 22 August 2006

Abstract—Two novel blue pigments, rosacyanins A1 and A2, were isolated from the petals of *Rosa hybrida* cv. ‘M’me. Violet’. Their structures were elucidated on the basis of high-resolution Fourier transform ion cyclotron resonance mass spectroscopy (HR-FT-ICR-MS), FABMS/MS/MS, ¹H, ¹³C and two-dimensional NMR. The molecular formulas of rosacyanin A1 (**1**) and A2 (**2**) are C₅₆H₃₇O₃₁ and C₆₃H₄₁O₃₅, respectively. The structures of rosacyanins A1 and A2 consisted of a common chromophore containing cyanidin with a galloyl group link between positions 4 and 5 of the hydroxyl group of the flavylum nucleus and tellimagrandins (1 or 2). These pigments in which anthocyanidin nuclei linked to ellagitannin through an ether bond are the first compounds isolated from natural sources.
© 2006 Elsevier Ltd. All rights reserved.

1. Introduction

Flower colour is mainly determined by the structures of anthocyanins. In particular, the structures of the chromophores, i.e., anthocyanidins, are important. Most blue flowers contain delphinidin-type anthocyanins, while orange to red flowers contain pelargonidin- and cyanidin-type anthocyanins.¹ Several factors in addition to anthocyanidin structure influence flower colour. It is well known that the bathochromic shift of anthocyanins is caused by their structure and interaction with co-existing compounds and the vacuolar pH.¹ The factors that contribute to the blue colour in flowers are (1) inter-molecular co-pigmentation with flavone or

flavonol,² as reported for *Iris ensata* Thunb.,³ (2) intra-molecular co-pigmentation, as observed in polyacylated anthocyanin, e.g., in *Gentiana makinoi*,⁴ *Ipomoea tricolor*,⁵ *Platycodon grandiflorum*,⁶ *Clitoria ternatea*,⁷ and *Senecio cruentus*,⁸ (3) high vacuolar pH, as in *Ipomoea tricolor* cv. ‘Heavenly Blue’,⁹ (4) formation of a metal complex¹⁰ (often called metallo-anthocyanin), such as commelinin isolated from *Commelina communis*¹¹ and *Hydrangea macrophylla*,¹² (5) the intra-molecular bonding of anthocyanidin and flavone in one molecule,^{13,14} and (6) the intra-molecular co-pigment and high vacuolar pH occurring in one *Petunia hybrida* mutant¹⁵ and a combination of these. Anthocyanins are usually stable under acidic conditions, when anthocyanins form a flavylum cation and exhibit red colour; on the other hand, under neutral and weakly acidic conditions, anthocyanins form a violet quinonoidal base¹ that is stabilised via intra-molecular co-pigmentation by polyacylation, as is the case for triacylated heavenly blue anthocyanin in *Ipomoea tricolor*⁵ and diacylated gentiodelphin in *Gentiana makinoi*.¹⁶

Hybridisation breeding of floricultural plants has contributed to increase the number of flower colour varieties. However, rose breeders have failed to obtain blue roses. Roses cannot synthesise delphinidin in their petals due to a deficiency of the flavonoid 3',5'-hydroxylase gene,¹⁷ which is critical to synthesise delphinidin. In addition, roses usually have low vacuolar pH and the anthocyanins in the petals

Keywords: Rose; *Rosa hybrida*; Rosacyanin; Anthocyanidin; Ellagitannin; Blue pigment; FABMS/MS/MS; ¹³C isotope shift.

Abbreviations: TFA, trifluoroacetic acid (CF₃COOH); TFA-*d*, CF₃COOD; DMSO-*d*₆, (CD₃)₂SO; MeOH, methanol; EtOH, ethanol; BuOH, *n*-butanol; HPLC, high-pressure liquid chromatography; *t*_R, retention time; FABMS, fast atom bombardment mass spectrometry; ESIMS, electro spray ionisation mass spectrometry; HR-FT-ICR-MS, high-resolution Fourier transform ion cyclotron resonance mass spectrometry; NMR, nuclear magnetic resonance; DQF-COSY, double quantum filtered correlation spectroscopy; NOESY, nuclear Overhauser and exchange spectroscopy; ROESY, rotating frame Overhauser enhancement spectroscopy; TOCSY, total correlation spectroscopy; ¹H{¹³C}-HSQC, ¹H{¹³C}-heteronuclear single quantum coherence; ¹H{¹³C}-HMBC, ¹H{¹³C}-heteronuclear multiple bond correlation; CD, circular dichroism; FTIR, Fourier transform infrared spectroscopy.

* Corresponding authors. E-mail addresses: yuko_fukui@suntory.co.jp; nomoto-core@rhythm.ocn.ne.jp

are rarely acylated, if at all; rose anthocyanins are pelargonidin/cyanidin 3-glucoside or 3,5-diglucoside, in which the cyanidin or pelargonidin was modified by one or two sugar molecules.¹⁸ Rose petals do not contain flavones, which have stronger co-pigment effects than the flavonols that roses accumulate. Therefore, roses lack the genetic background to become blue. Genetic engineering of roses makes it possible to generate varieties with a novel blue hue; these varieties express a heterologous F3'5'H gene and accumulate delphinidin almost exclusively.¹⁹ During our research for blue pigments from a large variety of roses, we found a small number of blue pigments (rosacyanin As) that mauve-type roses, such as 'M'me. Violet,' contain and have been studying their structure. In a previous study, we reported the structure of rosacyanin B,²⁰ which is a chromophore skeleton of rosacyanin As. The accumulation of rosacyanin As may be a better way to engineer blue roses than that of delphinidin, as rosacyanin As are consistently blue even when co-pigments and metal ions are absent and the vacuolar pH is low. In this paper, we reveal the unique structure of rosacyanin As, in which rosacyanin B and tannin bind together.

2. Results and discussion

2.1. Structural determination of rosacyanins A1 and A2

2.1.1. Structure of rosacyanin A1. Rosacyanin A1 (**1**) showed four absorption maxima in the UV–vis region [585 nm (log ϵ , 4.33), 424 nm (3.75), 354 nm (3.96) and 263 nm (4.65) in HCl/MeOH]. The addition of AlCl₃ to the MeOH solution caused a bathochromic shift of the λ_{\max} from 590 to 622 nm. This phenomenon of rosacyanin A1 is usually diagnostic of the presence of the *ortho* hydroxyl group in the B-ring. In the visible spectrum of **1**, the λ_{\max} and optical density of **1** at pH 1–8 are shown in Table 1. The λ_{\max} values were very different from those of typical anthocyanins, such as malvidin 3,5-diglucoside.²¹

In the positive mode, the FABMS of **1** showed a molecular ion at m/z 1205 [M]⁺ and in the negative mode, FABMS gave a molecular ion peak at m/z 1203 [M–2H][–]. The molecular formula of **1** was established on the basis of high-resolution Fourier transform ion cyclotron resonance mass spectra (HR-FT-ICR-MS), as C₅₆H₃₇O₃₁ was supported by a molecular ion peak at m/z 1205.13255 [M]⁺ (err. –1.009 ppm).

The ¹H NMR spectrum of **1** showed the duplication of each proton signal (totally 1H), which is characteristic of

Table 1. Change of the absorption maxima and optical densities of rosacyanin A1 in pH 1–8

pH	λ_{\max} (nm)	Optical density
1	567.0	0.1157
2	565.5	0.1274
3	557.5	0.1368
4	554.5	0.1455
5	555.0	0.1467
6	557.0	0.1390
7	564.0	0.1312
8	573.0	0.1392

The solution used for pH 1 and 2 was a Tris–HCl buffer and that for pH 3–8 was a McIlvaine buffer.

anomeric mixture formation.²² However, all proton signals in the sugar region of the two anomers were unambiguously distinguished from each other by ¹H–¹H COSY and the axial orientation of H-2, 3, 4 and 5, except for the anomeric proton H-1 (α -form: δ 5.30, J =2.0 Hz; β -form: δ 4.64, J =8.0 Hz) in the glucopyranose moiety, was evident from the coupling constant of the signals (Table 2).

Additionally, the H-6 methylene proton signals of the glucose moiety were observed at δ 3.60 and 5.03 in the α -anomer (δ 3.77 and 5.00 in the β -anomer) and the H-4 proton signal of the glucose moiety was observed at δ 4.87 in the α -anomer (δ 4.97 in the β -anomer). The H-6 proton had ¹H{¹³C}-HMBC cross peaks at δ 166.91 (Ha-7), while the H-4 proton had them at δ 167.64 (Hb-7'). The large difference in the chemical shift between geminal protons at the C-6 position is characteristic of an ellagitannin having an esterified hexahydroxydiphenoyl (HHDP) group at C-4/C-6 of the hydroxyl groups on the glucose moiety in many hydrolysable tannins.²² The Ha-3 (δ 6.29) and Hb-3' (δ 6.22) signals showed a cross peak with the carboxylic carbonyl carbon signals Ha-7 and Hb-7', respectively (Fig. 1).

Among the glucose proton signals, the H-2 and H-3 [δ 4.96 and 5.66 in the α -anomer (δ 4.83 and 5.51 in the β -anomer)] signals were shifted to a lower magnetic field from the corresponding glucose. In the ¹H NMR spectrum of **1**, the presence of two galloyl groups was revealed by the galloyl proton signals (δ 6.85, 6.78 each s, 2H in total and δ 6.78, 6.79 each s, 2H in total) with ¹H{¹³C}-HMBC correlation through carbonyl carbons (δ 165.11 and 165.40).

The enzymatic hydrolysis of **1** with tannase yielded degalloyl rosacyanin A1 (**4**). Its HR-FT-ICR-MS exhibited a molecular ion at m/z 901.10994 [M]⁺ and the molecular formula was C₄₂H₂₉O₂₃, losing two molecules of the galloyl moieties from the molecular ion of **1**.

In order to clarify all the proton signals of **1** and **4**, their NaBH₄ reduction gave the dihydro derivatives **5** and **6**, respectively (Scheme 1). HR-FT-ICR-MS of **5** and **6** exhibited a molecular ion at m/z 1207.14794 [M]⁺ (C₅₆H₃₉O₃₁) and 903.12406 [M]⁺ (C₄₂H₃₁O₂₃), respectively. These products, **5** and **6**, allowed a straightforward structural elucidation in the NMR spectrum. The assignments of the ¹H and ¹³C signals of **5** and **6** are shown in Tables 2 and 3.

For further details of the structural determination, ¹H{¹³C}-HMBC of compound **6** was measured, and its network and numbering of atoms are shown in Figure 2. Thus, the 1H singlet proton signal (δ 6.28) due to Hb-3' showed a cross peak with the ester carbonyl carbon Hb-7' signals (δ 170.56) on the same ring and the Ha-1 aromatic carbon signal (δ 115.67) of the neighbouring Ha benzene. On the other hand, the 1H singlet proton signal (δ 6.69) due to Ha-3 also observed a cross peak with the Ha-7 carbon signal (δ 169.36) and the Hb-1' carbon (δ 115.91), indicating that two gallate moieties formed an HHDP group by connecting with a C–C bond. In addition, two carboxylic carbonyl carbons (δ 169.36 and 170.56) of the HHDP group correlated through three-bond coupling with the H-4 proton (δ 4.74) and H-6 methylene protons (δ 4.39 and 3.66) on the glucitol moiety, suggested

Table 2. ^1H NMR assignment of compounds **1**, **2**, **5**, **6** and **7**

	1 : α -form	1 : β -form	2	5	6	7
Chromophore						
A-6	6.82d (2)	6.81	6.84d (2)	6.82br s	6.28 (1)	6.89d (1)
A-8	6.98d (2)	6.98	7.04d (2)	7.01br s	6.36d (1)	7.06d (1)
B-2'	8.33d (2)	8.34	8.32d (2)	8.32br s	7.63d (2)	8.14br s
B-5'	6.96d (8)	6.96	6.97d (8)	6.96d (8)	6.60d (8)	6.92d (9)
B-6'	8.10dd (2, 8)	8.10	8.08dd (2, 8)	8.07d (8)	7.65dd (2, 8)	8.11dd (1, 9)
D-3''	6.80s	6.80	6.78s	6.77s	6.49s	6.85s
HHDP						
Ha-3	6.29s	6.26s	6.26s	6.72s	6.69s	7.17s
Hb-3'	6.22s	6.22s	6.23s	6.13s	6.28s	7.56s
Glucose						
1 (a)	5.30d (2)	4.87d (8)	6.14d (8)	Glucitol	Glucitol	
1b				3.73br d (8)	3.54dd (4, 13)	
2	4.96dd (2, 9)	4.83t (9)	5.34dd (8, 10)	3.62br d (8)	3.45m	
3	5.66t (10)	5.51t (10)	5.76t (10)	5.12br d (8)	3.52dd (4, 5)	
4	4.87t (10)	4.97t (10)	4.92t (10)	5.79d (8)	3.71dd (1.5, 5)	
5	4.49dd (7, 10)	4.28dd (7, 10)	4.59ddd (2, 6, 10)	5.05d (8)	4.74dd (1.5, 8.5)	
6a	5.03dd (7, 12)	5.00dd (7, 12)	5.04dd (6, 12)	3.80d (8)	4.11dd (2, 8.5)	
6b	3.67d (12)	3.77br d (12)	3.76dd (2, 12)	4.24br d (12)	4.39dd (2, 13)	
				3.68br d (12)	3.66d (13)	
GA						
GA1-2,6			6.87s			
GA2-2,6	6.85s	6.79s	6.796s	6.85s		
GA3-2,6	6.78s	6.78s	6.805s	6.78s		

Chemical shift in δ (J in hertz). Compounds **1**, **2**, **5** and **7** were measured in DMSO- d_6 containing 1% DCl and compound **6** was measured with coaxial tube in $\text{CD}_3\text{CN}:\text{D}_2\text{O}:\text{TFA}-d=50:50:0.5$ (inner tube)/ $\text{CD}_3\text{CN}:\text{H}_2\text{O}:\text{TFA}=50:50:0.5$ (outer tube).

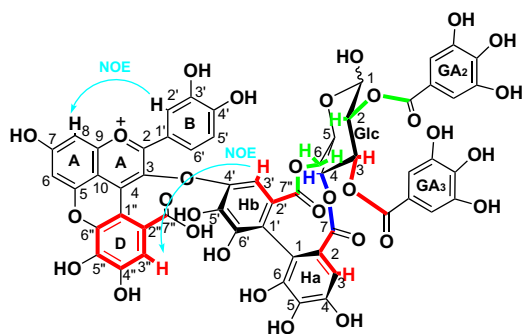


Figure 1. Structure of compound **1** with HMBC and NOE. The significant HMBCs are shown in coloured bonds. NOE is shown with arrows. Atom numbers are shown on each atom.

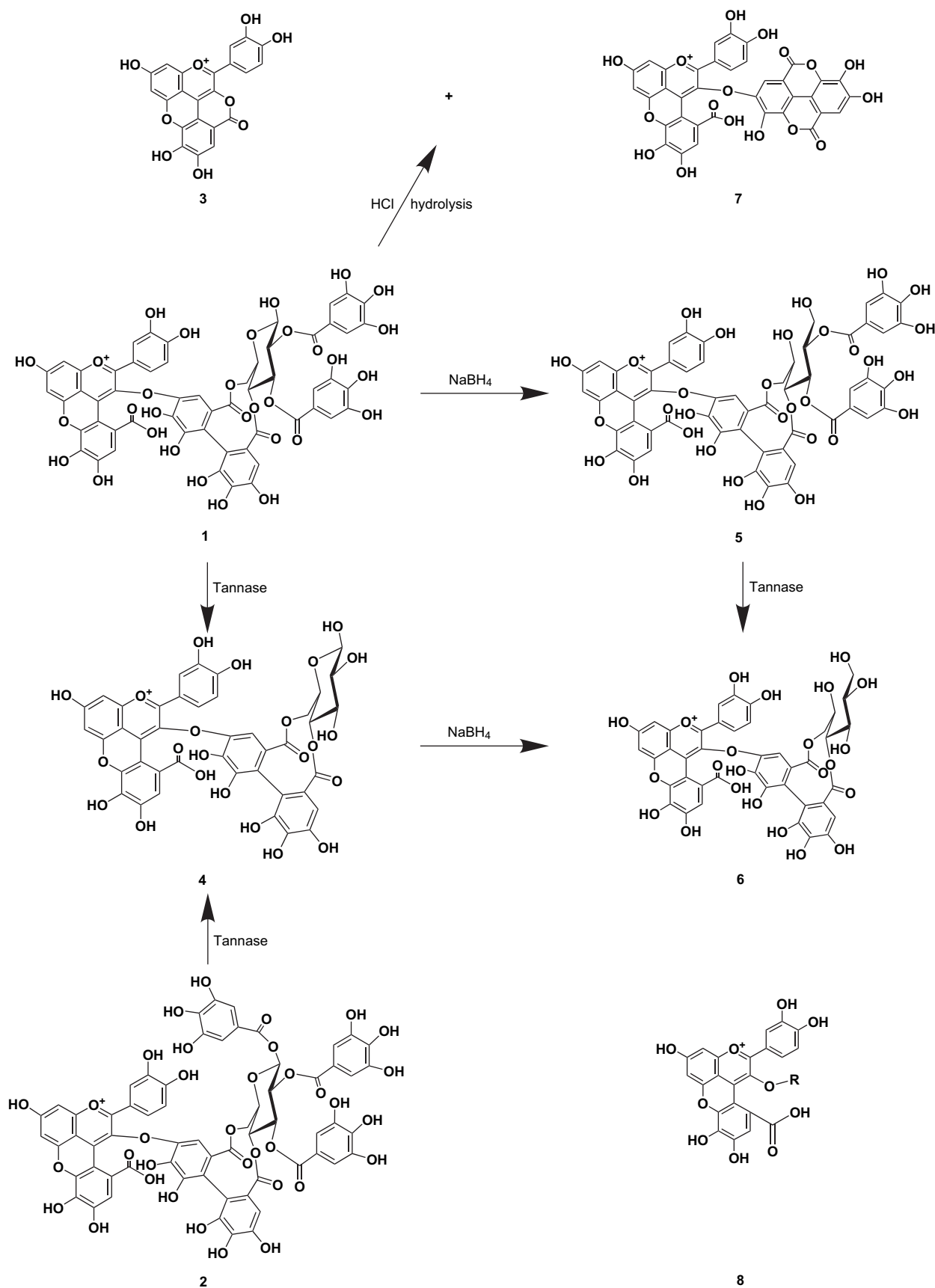
that **1** has a kind of ellagitannin, the tellimagrandin **1**^{23,24} moiety.

The findings described above were also supported by FABMS/MS fragment ions at m/z 721 generated by cleavage, as shown in Figure 3. In addition to the above-mentioned proton signals, five of the six ^1H proton signals in the aromatic region were attributed to H-6 (δ 6.82, d, 2) and H-8 (δ 6.98, d, 2) in the A ring and H-2' (δ 8.33, d, 2), H-5' (δ 6.96, d, 8) and H-6' (δ 8.10, dd, 2, 8) in the B-ring of the flavylum form of the cyanidin nucleus. The low-field singlet (δ 8.60–9.10) characteristic of the H-4 of anthocyanidin was missing in the spectrum of **1**. In the $^1\text{H}\{^{13}\text{C}\}$ -HMBC spectrum of **1**, the remaining proton signal (D-3'': δ 6.80, s) showed cross peaks with five carbon signals of a benzene ring and the carbonyl carbon signal at δ 166.17 (Fig. 1) as well as with rosacyanin B.

FABMS/MS for the molecular ion m/z 1205 $[\text{M}]^+$ showed fragment ion peaks at m/z 153, 420, 721 and 1053, and the

prominent ion at m/z 420 generated the ether bond cleavage between the C-3 of cyanidin in the chromophore and tellimagrandin **1** moiety, as shown in Figure 3 (Supplementary Fig. 1). FABMS/MS/MS of **1** for the ion at m/z 420 gave fragment ion peaks at m/z 137 and 109; these were the same as those observed in the FABMS/MS spectrum of rosacyanin B²⁰ or flavone.²⁵ These facts suggested that the C-4 position of the cyanidin nucleus in **1** was substituted with the gallic acid moiety as in rosacyanin B. Therefore, these results indicated that **1** consisted of a cyanidin nucleus with C-4 gallate (the chromophore part) and tellimagrandin **1** (the tannin part).

In order to determine the linkage position of the chromophore and tannin parts, we assigned all of the ^1H and ^{13}C NMR signals of **6** using $^1\text{H}\{^{13}\text{C}\}$ -HSQC, $^1\text{H}\{^{13}\text{C}\}$ -HMBC, TOCSY and DQF-COSY, as shown in Tables 2 and 3. Next, a deuterium-induced ^{13}C isotope shift experiment of **6** in 50% $\text{CD}_3\text{CN}/\text{D}_2\text{O}$ with TFA- d and 50% $\text{CD}_3\text{CN}/\text{H}_2\text{O}$ with TFA was carried out. All carbon signals bearing the hydroxyl or phenolic hydroxyl group were observed as a doublet with an isotope shift, except for two singlet carbon signals at δ 145.06 due to A-3 of the cyanidin nucleus and at δ 146.97 attributed to Hb-4 of the HHDP group (Supplementary Fig. 2). In addition, the D-7 carboxy-carbonyl carbon signal at δ 167.57 appeared as a doublet peak and shifted to a lower magnetic field than that in rosacyanin B (δ 156.67). In the FTIR spectrum of **1**, rather than the disappearance of a peak due to the α -pyrone ring at 1725 cm^{-1} that was noted in rosacyanin B, a peak attributed to the carboxylic group was observed at 1707 cm^{-1} . In the NOESY spectrum of **6**, the NOE correlation of the signal of D-3'' with the signal of Hb-3' of the HHDP moiety suggested a spatial proximity of the D gallery ring to Hb of HHDP (Fig. 4). In addition, the 6 N-HCl hydrolysis of **1** gave gallic acid, cyanidin, rosacyanin B and an unknown blue pigment



Scheme 1. Structure of rosacyanins and their derivatives: **1**, rosacyanin A1; **2**, rosacyanin A2; **3**, rosacyanin B; **4**, degalloyl rosacyanins A1 and A2; **5**, NaBH₄ reduced rosacyanin A1; **6**, degalloyl NaBH₄ reduced rosacyanin A1; **7**, HCl hydrolysed rosacyanin A1; **8**, chromophore moiety of rosacyanins A1 and A2.

Table 3. ^{13}C NMR assignment of compounds **1**, **2**, **5**, **6** and **7**

	1 (α -form)	2	5	6	7	
Chromophore						
A-2	156.76	156.53	156.56	157.79s	156.7	
A-3	145.30	145.16	145.17	145.06s	145.3	
A-4	132.13	131.88	132.03	131.06s	131.9	
A-5	149.94	149.76	149.84	150.19s	150.2	
A-6	99.41	99.20	99.29	100.33s	99.1	
A-7	162.66	162.49	162.63	163.12s	163.0	
A-8	96.77	96.58	96.65	97.68s	96.4	
A-9	150.87	150.71	150.79	151.20s	150.9	
A-10	106.50	106.35	106.38	106.86s	106.5	
B-1'	122.31	122.13	122.15	123.20s	122.2	
B-2'	117.61	117.08	117.17	117.63s	116.9	
B-3'	144.59	145.00	144.36	145.15d	145.4	
B-4'	151.22	150.91	151.07	151.46d	151.2	
B-5'	116.18	115.58	116.79	116.43s	115.1	
B-6'	123.87	123.28	123.70	126.12s	124.2	
D-1''	113.37	111.21	111.19	113.58s	111.6	
D-2''	111.37	111.21	111.19	112.53s	111.6	
D-3''	101.80	101.50	101.60	104.79s	101.7	
D-4''	150.30	150.13	150.10	151.11d	151.4	
D-5''	139.74	139.27	140.03	140.66d	139.0	
D-6''	139.14	136.69	139.17	138.47s	138.7	
D-7''	166.17	166.01	166.13	167.57d	165.8	
HHDP						
Ha-1	115.00	114.78	115.36	115.67s	114.2	
Ha-2	123.72	123.65	a 123.03	125.16s	123.1	c
Ha-3	105.39	105.19	106.38	108.83s	109.5	
Ha-4	144.59	144.25	144.36	145.41d	148.5	
Ha-5	135.37	135.12	135.58	136.71d	140.6	
Ha-6	144.72	144.53	b 145.10	144.56d	145.9	d
Ha-7	166.91	166.71	167.07	169.36s	159.1	
Hb-1'	117.30	117.55	116.07	115.91s	111.8	
Hb-2'	123.60	123.43	a* 124.70	126.82s	123.8	c*
Hb-3'	104.48	104.64	103.79	104.7s	110.5	
Hb-4'	145.64	145.33	144.73	146.97s	148.6	
Hb-5'	136.70	139.68	136.01	136.28d	139.4	
Hb-6'	144.59	144.38	b* 145.10	144.8d	146.9	d*
Hb-7'	167.64	167.27	168.75	170.56s	158.9	
Glucose						
	\cong -form					
1	89.73	91.87	59.14	63.29d		
2	72.17	70.39	72.88	72.91d		
3	69.90	71.58	69.61	69.96d		
4	70.22	69.52	72.07	75.83s		
5	65.68	71.03	66.97	68.35d		
6	62.65	61.85	67.47	68.87s		
GA (Glc-2,3)						
GA2-1	118.76	118.0	118.90			
GA2-2,6	108.89	108.74	108.80			
GA2-3,5	145.51	145.07	145.17			
GA2-4	138.76	138.79	138.21			
GA2-C=O	165.11	164.22	165.10			
GA3-1	118.77	117.83	119.38			
GA3-2,3	108.82	108.61	108.90			
GA3-3,5	145.30	145.25	145.26			
GA3-4	138.93	138.60	138.46			
GA3-C=O	165.40	165.01	165.40			
Glucose						
	\cong -form	GA1 (Glc-1)				
1	95.1	GA1-1 117.20	a and a*, b and b*, c and c*, d and d*, these signals may be interchangeable with each other.			
2	70.2	GA1-2,6 108.86				
3	72.2	GA1-3,5 145.39				
4	73.1	GA1-4 139.08				
5	70.2	GA1-C=O 163.80				
6	62.6					

Chemical shift in δ . Compounds **1**, **2**, **5** and **7** were measured in $\text{DMSO}-d_6$ containing 1% DCl and compound **6** was measured in $\text{CD}_3\text{CN}/\text{D}_2\text{O}$ containing TFA-*d*. In the chemical shift of compound **1** in the β -form, only the glucose moiety is distinguishable. In compound **6**, s means singlet and d means doublet in the isotope shift.

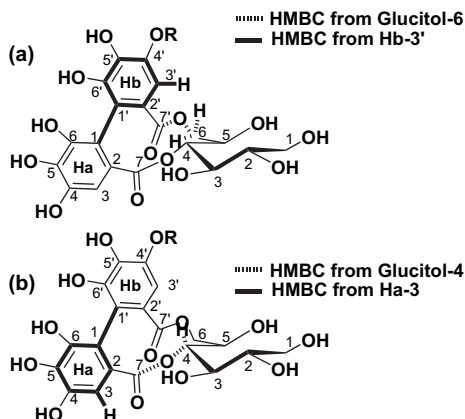


Figure 2. Long-range HMBC of **6** in the tannin part. (a): The HMBCs from the Hb-3' proton are shown in thick lines, (b): the HMBCs from the Ha-3 proton are shown in thick lines. Both protons have cross peaks to the C-1 carbon on the opposite benzene.

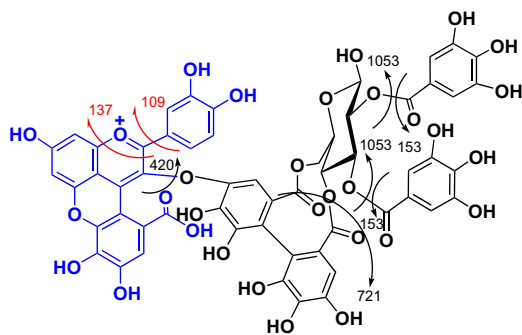


Figure 3. FABMS/MS and MS/MS/MS assignments of **1**. Black arrows show the MS/MS assignment from m/z 1205 and red arrows show the MS/MS/MS assignment from m/z 420.

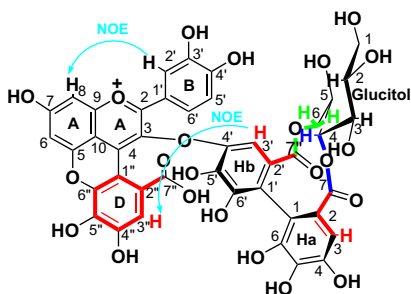


Figure 4. HMBC and NOE of compound **6**. The significant HMBCs are shown in coloured lines. NOE is shown with arrows. Atom numbers are shown on each atom.

(**7**), which had λ_{\max} of 590 nm in 90% CH_3CN with 0.5% TFA. ESIMS of **7** exhibited molecular ions at m/z 721 $[\text{M}]^+$, losing two molecules of the galloyl groups, two H_2O molecules and one glucose molecule from the molecule of **1**. In the ^1H NMR spectrum of **7**, all proton signals were only observed in the aromatic region, namely, two proton signals due to the ellagic acid group (δ 7.17, s and 7.56, s), five *ortho*- and *meta*-coupled signals attributed to the flavylum nucleus (δ 6.89, d, $J=1$; 7.06, d, $J=1$; 8.14, br s; 6.92, d, $J=9$; 8.11, dd, $J=9.1$) and one additional proton signal assigned to D-3 on the galloyl moiety (δ 6.85, s). Furthermore, the chemical shifts of two carbonyl carbons (δ 159.14 and 158.92) coincided with those of α -pyrone ring systems,

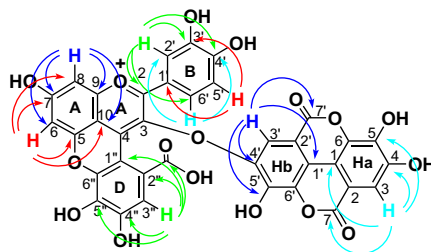


Figure 5. HMBC of compound **7**. The HMBC network of compound **7** is shown with curved arrows.

such as rosacyanin B²⁰ and ellagic acid.²⁶ The $^1\text{H}\{^{13}\text{C}\}$ -HMBC spectrum supported the structure of **7**. Thus, the structure of **7** was illustrated by the formula with the HMBC network shown in Figure 5.

In the CD spectrum, **1** has a positive cotton effect at around 260 nm, similarly to tellimagrandin **1**; therefore, the HHDP moiety has an *S* configuration, which is the same as tellimagrandin **1**. Considering the results reported above, the structure of rosacyanin A1 was proposed to be **1**, as shown in Figure 1.

2.1.2. Structure of rosacyanin A2. The UV–vis spectrum of rosacyanin A2 (**2**) is very similar to that of **1** and had λ_{\max} 585 nm. The molecular formula of **2** was determined to be $\text{C}_{63}\text{H}_{41}\text{O}_{35}$ on the basis of a molecular ion at m/z 1357.144794 $[\text{M}]^+$ (err. -1.633 ppm) in its HR-FT-ICR-MS. The molecular ion at m/z 1357 $[\text{M}]^+$ increased 152 mass units, corresponding to one molecule of the galloyl group, compared to the peak of the molecular ion of **1** at m/z 1205 $[\text{M}]^+$. In the positive mode, FABMS/MS of **2** from m/z 1357 gave a fragment ion at m/z 420, which was the same chromophore (**8**) as rosacyanin A1. The ^1H and ^{13}C NMR spectra of **2** indicated the presence of chromophore (**8**), three galloyl groups, an HHDP and a glucose moiety. In ^1H NMR, the anomeric proton of **2** was observed as a doublet with a coupling constant of 8 Hz at δ 6.14 demonstrating that an additional β -oriented galloyl group in **2** was substituted at the C-1 position on the glucose moiety. Moreover, the tannase hydrolysis of **2** yielded degalloyl rosacyanin A1 (**4**). This finding and the NMR result (Tables 2 and 3) suggested that the structure of **2** was gallate-esterified at C-1 of the glucose moiety. The tannin part of **2** was identified as tellimagrandin **2**.²³ In the CD spectrum, **2** has a positive cotton effect around 260 nm and the HHDP moiety has an *S* configuration that is identical to that of tellimagrandin **2**. Finally, the structure of rosacyanin A2 was established as **2**, as shown in Figure 6.

2.2. Properties of rosacyanins

Since both rosacyanins (**1** and **2**) have their 4-position substituted, it is predicted that this substitution affects the properties of these rosacyanins in a neutral or weakly acidic aqueous solution. This is because the substitution at position 4 of the flavylum cation affects the distribution of the charge throughout the molecule and, as a result, positions 2 and 4 become less reactive to the nucleophilic attack.²⁷ Thus, the presence of a 4-substituent on the cyanidin nuclei provides great resistance to hydration at the 2-position; in other words, it increases the stability of the anthocyanidin nuclei.

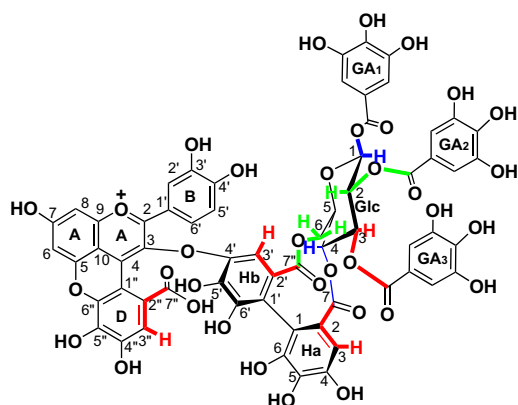


Figure 6. Structure and HMBC of rosacyanin A2 (**2**). The significant HMBCs are shown in coloured lines. Atom numbers are shown on each atom.

Under acidic condition ($\text{pH} < 2$), the flavylium cation form (Fig. 7a1) and the pyrylium cation form (Fig. 7a2) are predominant, whereas under weakly acidic conditions (pH 3–6), the opposite is true, i.e., it displays a violet quinonoidal

form (Fig. 7b1–3). Above pH 7, a quinonoidal base anion structure (Fig. 7c1–3) that is blue in colour is formed. In the pH range of 3–6, the λ_{max} of rosacyanin shifted from 567 to 555 nm. An explanation for this hypochromic effect may be that the positive charge on the flavylium ring may be delocalised by resonance and reside largely on the oxygen atom on the newly formed pyrylium ring (Fig. 7a1). Thus, the chromophore of rosacyanin has many resonance forms to inhibit hydration at the 2-position, which is the hydrobase.

In general, simple anthocyanins, mono- or diglucoside, are red or orange at low pH ; however, under weakly acidic conditions, their 2-positions are easily hydrated and become colourless pseudobases. Rosacyanins are blue or violet in a wide pH range (pH 1–7). A possible explanation for the bluing mechanism of rosacyanin molecules may be that they form a horizontally or vertically stacked molecule. No NOE, however, was observed at the signals of the tellimagrandin 1 moiety between the cyanidin nuclei, but NOE was observed between A-8 and B-2''/B-6'', suggesting that the protons on the cyanidin nucleus and tellimagrandin 1

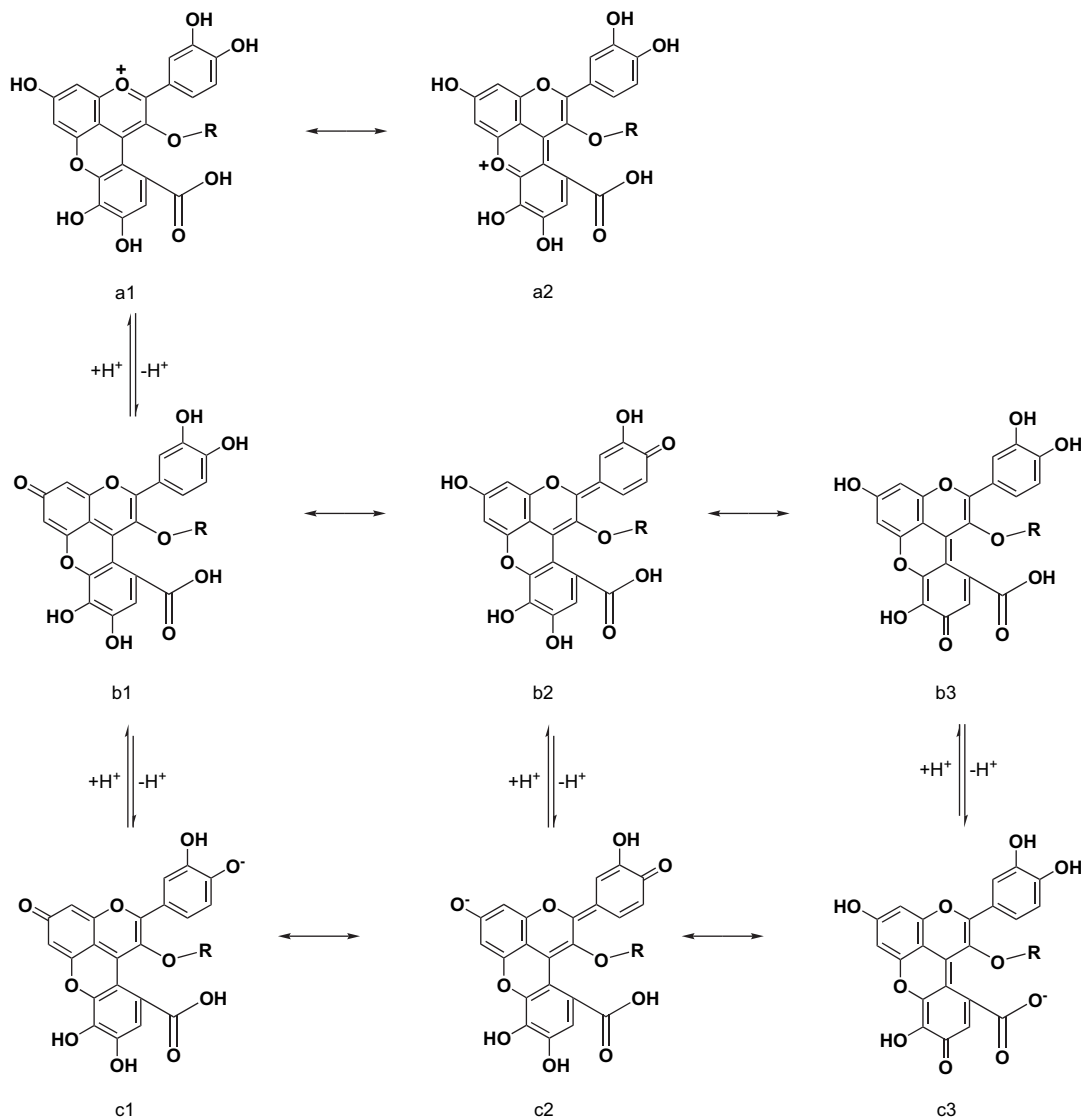


Figure 7. Possible mesomeric forms of the chromophore of rosacyanin: a1, flavylium cation; a2, pyrylium cation; b, quinonoidal base; b1, A7 oxo-type; b2, B4' oxo-type; b3, D4'' oxo-type; c, quinonoidal base anion; c1, A7 oxo-type; c2, B4' oxo-type; c3, D4'' oxo-type.

are located at a greater distance than A-8 and B-2''/B-6'' (Fig. 1). Therefore, the chromophore of rosacyanins is considered to have no intra-molecular stacking with any aromatic ring in the HHDP and galloyl groups of the tellimagrandin 1 moiety.

2.3. Conclusion

We have found mauve roses containing a small amount of blue pigments co-existing with a red anthocyanin and cyanidin 3,5-diglucoside, and determined that the coexistence of a small quantity of the present blue pigments (rosacyanins) is the reason that the roses look bluish. These pigments are called 'rosacyanin' because of their true blue colour and they were isolated from the petals of *Rosa hybrid* cv. 'M'me. Violet'.

Rosacyanins **1** and **2** had a common chromophore, which contained cyanidin with a galloyl group link between positions 4 and 5 of the hydroxy group of the flavylum nucleus, and tellimagrandin 1 and 2, respectively, at C-3 of cyanidin nucleus.

To our knowledge, this is the first natural pigment in which the flavylum nucleus binds to ellagitannin but not through sugar. Similar compounds, including tannins, are known and have been isolated from *Camellia japonica* L.,²⁸ *Quercus* and *Castanopsis asicies*,^{29,30} in which the sugar moieties of ellagitannins bind to catechin by the C–C bond.

The HCl hydrolysis product (**7**) of **1** has λ_{\max} 590 nm and is still blue. When the bluish polyacylated anthocyanins isolated hitherto, such as gentiodelphin,¹⁶ were compared with rosacyanins (**1** and **2**) or **7**, the bathochromic shift of the latter pigments was not explained as former pigments result from the stacking of the chromophore and tannin moieties. This is because no NOE was observed between the signals of the cyanidin nucleus proton between the tellimagrandin moieties. From now on, detailed studies will be conducted to elucidate the bluish mechanism on rosacyanins and their derivative molecules.

Rosacyanins, which not only are 4-substituted but also have their 5 position substituted, showed a greater resistance to hydration, a greater colour expression at higher pH values and increased stability of the molecules. Rosacyanins are thought to be biosynthesised by an enzymatic cycloaddition or by a nucleophilic and electrophilic addition of cyanidin with a large amount of tellimagrandin 1 and 2 distributed in the rose petals.^{31,32} It is very interesting that cyanidin changed to blue by binding to tellimagrandin, although the change cannot be attributed to coexistence with tellimagrandin 1, but with pentagalloyl-glucose.^{32,33} The accumulation of a large amount of rosacyanins in the petals will result in a blue rose.

3. Experimental

3.1. General

Compounds **1**, **2**, **5** and **7** were dissolved in DMSO-*d*₆ containing 1% DCl and compound **6** was dissolved in 50% CD₃CN/D₂O containing 0.5% TFA-*d*; ¹H NMR, ¹³C NMR,

¹H{¹³C}-HSQC, ¹H{¹³C}-HMBC, TOCSY, DQF-COSY and NOESY spectra were obtained on an AVANCE-750 spectrometer (BRUKER BIOSPIN, Germany). The method used for the ¹H{¹³C}-HMBC measurement to observe a long-range spin–spin coupling between a proton and a carbon is shown below. To observe a long-range spin–spin coupling between a proton and a carbon, the delay for the evolution of small couplings in the gradient-enhanced HMBC pulse sequence was set to 300 ms. This value optimises the observation at around 1.7 Hz of the spin–spin coupling constant, whereas the usual HMBC delay parameter was set to 65 ms, which is focused on the coupling constant 8 Hz.

The deuterium induced a differential ¹³C isotope shift³⁴ that was obtained with a dual sample tube consisting of an inner tube (2.9 mmϕ) with 0.11 mM of **6** in 50% CD₃CN/D₂O with 0.5% TFA-*d* and an outer tube (5 mmϕ) with 0.11 mM of **6** in 50% CD₃CN/H₂O with 0.5% TFA. ¹³C NMR was measured on a DMX-500 spectrometer (BRUKER BIOSPIN, Germany). The residual proton peaks and ¹³C peaks of CD₃CN (δ 1.94 for ¹H and δ 1.36: CD₃ and 118.32: CN for ¹³C) or DMSO-*d*₆ (δ 2.50 for ¹H and δ 39.43 for ¹³C) were used as the internal standard (the assignment of data are shown in Tables 2 and 3).

Fast atom bombardment mass spectra (FABMS) and FABMS/MS or FABMS/MS/MS of **1** and **2** were recorded on a JMS-HX110/HX110A tandem mass spectrometer (JEOL, Japan) in the positive mode with a nitrobenzylalcohol matrix. The ESIMS of **7** was obtained by Q-TOF with a z-spray ion source (Micromass, Manchester, UK) in the positive mode. High-resolution mass spectra (HRMS) of **1**, **2**, **4**, **5** and **6** were recorded on a 9.4T FT-ICR MS APEX-Q spectrometer (BRUKER Daltonics, Germany) with an Apollo ESI ion source in the positive mode.

Compounds **1**, **2**, **4** and **6** were dissolved in MeOH containing 0.1% HCl (0.02 mM) and the UV–vis spectrum was measured at 700–200 nm. Compound **1** was diluted with pH 1–8 in 0.01 mM buffers and the visible spectra at 780–400 nm were measured with a 5-cm light-pass crystal cell. The solution used for pH 1 and 2 was a 0.1 M Tris–HCl buffer, and that for pH 3–8 consisted of a McIlvaine buffer prepared with 0.1 M citric acid and 0.2 M Na₂HPO₄ (Table 1). Compound **1** (86 µg) was dissolved in 5 mL of MeOH (0.0143 mM) and the UV–vis spectrum was measured; then, a 1% AlCl₃ solution was added and the UV–vis spectrum was measured at 780–250 nm. These analyses were conducted using a Shimadzu UV-2500PC spectrophotometer (Shimadzu Corporation, Japan).

The FTIR spectra of **1** and **2** were measured on a Nicolet 710 FT-IR with single-reflection ATR using a diamond crystal.

The CD spectra of **1**, **2** and **5** were measured on a J-725 spectropolarimeter (Jasco Corporation, Japan) in MeOH (0.1 mM) with a 1 mm crystal cell.

3.2. Materials

Rosa hybrida cv. M'me. Violet, purchased from the Tsukimoto Rose Garden (Kyoto, Japan), was grown in a typical greenhouse.

3.3. Purification of rosacyanins

Petals of *Rosa hybrida* cv. 'M' me. Violet' (7.9 kg) upon storage at -80°C were pulverised in liquid N_2 and extracted with 15 L of 80% aqueous acetonitrile containing 0.1% TFA. After filtration, the extract was concentrated under vacuum and applied on a Sephadex LH-20 (9 L, Pharmacia Biotech, Sweden) column and eluted step-wise with 30% CH_3CN containing 0.1% TFA and 60% CH_3CN .

The 60% CH_3CN fraction was separated into two fractions; the former fraction was concentrated under vacuum and applied on HP-20 (1.5 L, Mitsubishi Chemical Co., Ltd, Japan). The column was washed with 2 L of H_2O and then eluted with 3 L of 10% CH_3CN containing 0.1% TFA and 3 L of 50% CH_3CN containing 0.1% TFA step-wise. The fraction including rosacyanin A1 (**1**) was eluted with 50% CH_3CN fraction.

This fraction was purified by preparative HPLC as below. The HPLC was accomplished with the use of a Develosil-ODS-UG-15/30 (50 cm \times 5 cm, Nomura Chemical, Ltd, Japan) column with a flow rate of 32 mL/min and the absorbance was monitored at 260 nm. The solvent system used included gradient elution for 80 min using 30–100% of solvent B (50% $\text{CH}_3\text{CN}/\text{H}_2\text{O}$, 0.5% TFA) in solvent A (0.5% TFA/ H_2O).

The fraction including **1** was further purified using a Sephadex LH-20 (600 mL, Pharmacia Biotech, Sweden) column with 50% $\text{CH}_3\text{CN}/\text{H}_2\text{O}$. After 1.5 L elution, rosacyanin A1 was eluted. This fraction was finally applied on the HPLC using a YMC-pack Polymer C18 (30 cm \times 2 cm, YMC Co., Ltd, Japan) with a flow rate of 6 mL/min and monitoring by UV Abs. at 260 nm. The solvent system used was as follows: after 30 min of isocratic elution with 70% solvent B, gradient elution for 20 min using 70–90% of solvent B (50% $\text{CH}_3\text{CN}/\text{H}_2\text{O}$, 0.5% TFA) in solvent A (0.5% TFA/ H_2O) was carried out. After these chromatograms, 80 mg of **1** was obtained.

The latter 60% CH_3CN fraction of the first LH-20 column chromatogram was purified by preparative HPLC as below. The HPLC was accomplished by using a Develosil-ODS-UG-15/30 (50 cm \times 5 cm, Nomura Chemical, Ltd, Japan) column with a flow rate of 32 mL/min and monitoring at A260 nm. The solvent system used included gradient elution for 80 min using 40–100% of solvent B (50% $\text{CH}_3\text{CN}/\text{H}_2\text{O}$, 0.5% TFA) in solvent A (0.5% TFA/ H_2O).

The fraction including rosacyanin A2 (**2**) was applied on the HPLC using a YMC-pack Polymer C18 (30 cm \times 2 cm, YMC Co., Ltd, Japan) column with a flow rate of 6 mL/min and monitoring at A260 nm. The solvent system used was as follows: after 30 min of isocratic elution with 75% solvent B, gradient elution for 20 min using 75–100% of solvent B (50% $\text{CH}_3\text{CN}/\text{H}_2\text{O}$, 0.5% TFA) in solvent A (0.5% TFA/ H_2O) was carried out. The fraction including **2** was finally applied on the HPLC using a Develosil C30-UG-5 (30 cm \times 2 cm, Nomura Chemical, Ltd, Japan) column with a flow rate of 6 mL/min and monitoring at A260 nm. The solvent system used was as follows: after 30 min of isocratic elution with 70% solvent B, gradient elution for 20 min

using 70–90% of solvent B (50% $\text{CH}_3\text{CN}/\text{H}_2\text{O}$, 0.5% TFA) in solvent A (0.5% TFA/ H_2O) was carried out. After these chromatograms, 8 mg of **2** was obtained.

3.3.1. Rosacyanin A1 (1). Blue amorphous powder. IR ν_{max} : 1707, 1606, 1327, 1191, 1028 cm^{-1} ; UV-vis (0.1% HCl/MeOH) λ_{max} : 585 (log ϵ , 4.26), 424 (3.753), 354 (3.950), 263 (4.581) and 216 nm (4.87); CD (MeOH): $[\theta]_{284} +1.23 \times 10^4$, $[\theta]_{261} -1.00 \times 10^4$, $[\theta]_{232} +1.88 \times 10^4$; FABMS/MS m/z : 1205, 1053, 721, 420, 153; HR-FT-ICR-MS: 1205.13255 calculated for $\text{C}_{56}\text{H}_{37}\text{O}_{31}$ (1205.13133, err. -1.009 ppm); ^1H and ^{13}C NMR (1% DCl/DMSO- d_6): Tables 2 and 3.

3.3.2. Rosacyanin A2 (2). Blue amorphous powder. IR ν_{max} : 1719, 1603, 1321, 1185, 1020 cm^{-1} ; UV-vis (0.1% HCl/MeOH) λ_{max} : 585 (log ϵ , 3.74), 267 (4.51) and 216 nm (4.87); CD (MeOH): $[\theta]_{281} +6.84 \times 10^3$, $[\theta]_{256} -4.28 \times 10^3$, $[\theta]_{225} +1.29 \times 10^4$; FABMS/MS m/z : 1053, 721, 420, 153; HR-FT-ICR-MS: 1357.14451 calculated for $\text{C}_{63}\text{H}_{41}\text{O}_{35}$ (1357.14229, err. -1.633 ppm); ^1H and ^{13}C NMR (1% DCl/DMSO- d_6): Tables 2 and 3.

3.4. HCl hydrolysis of 1

Rosacyanin A1 **1** (8 mg) was hydrolysed in 25 mL of 6 N HCl at 100°C for 18 min. The hydrolysate was extracted with 4 mL of BuOH and the organic layer was purified by reverse-phase HPLC using a Polymer C18 (2 cm ϕ \times 30 cm, YMC Co., Ltd, Japan) column to obtain four fractions. Fraction A was gallic acid, fraction B was cyanidin and fraction C was Rosacyanin B, as determined by HPLC and TOFMS analysis and their molecular ions at m/z 169 $[\text{M}-\text{H}]^-$, m/z 287 $[\text{M}]^+$ and m/z 419 $[\text{M}]^+$, respectively. Fraction D (**7**) contained 1.8 mg of blue pigment, which has λ_{max} of 590 nm in 90% CH_3CN with 0.5% TFA, and its structure was determined by TOFMS and NMR analyses.

3.5. Enzymatic hydrolysis of 1

The enzymatic hydrolysis of 30 mg of **1** was performed with 20 mg of tannase (Kikkoman Co., Ltd) in 100 mL of 0.1 M potassium phosphate buffer, pH 5.5, at room temperature for 24 h. The reactant was purified using Superdex Peptide HR10/30 (1 cm ϕ \times 30 cm, Pharmacia Biotech, Sweden) with 50% $\text{CH}_3\text{CN}/\text{H}_2\text{O}$ containing 0.01% TFA to yield 15 mg of hydrolysate (**4**). In the same procedure, **4** was obtained from **2**.

3.5.1. Degalloyl rosacyanin A1 (4). Blue amorphous powder. UV-vis (0.1% HCl/MeOH) λ_{max} : 585 (log ϵ , 4.40), 360 (4.02), 260 (sh, 4.56) and 211 nm (4.83); CD (MeOH): $[\theta]_{282} +5.93 \times 10^3$, $[\theta]_{259} -1.16 \times 10^4$, $[\theta]_{216} +1.41 \times 10^4$, HR-FT-ICR-MS: 901.10994 calculated for $\text{C}_{42}\text{H}_{29}\text{O}_{23}$ (901.10941, err. -0.585 ppm).

3.6. NaBH_4 reduction of 1 and 4

NaBH_4 (120 mg) was added to a solution of 60 mg of **1** in 100 mL MeOH; the reaction mixture was left for 30 min and then 15 mL of 1 N HCl was added to it. The reactant was purified by reverse-phase HPLC using a Polymer C18 (2 cm ϕ \times 30 cm, YMC Co., Ltd, Japan) column to obtain 24 mg of **5**. Compound **4** (15 mg) was reduced in the same

manner as for **1** to obtain 6 mg of **6**. The structures of the derivatives of **1** are shown in Scheme 1.

3.6.1. Reduced rosacyanin A1 (5). Blue amorphous powder. UV–vis (0.1% HCl/MeOH) λ_{max} : 587 (log ϵ , 4.03), 260 (4.45) and 214 nm (4.83); HR-FT-ICR-MS: 1207.14794 calculated for $\text{C}_{56}\text{H}_{34}\text{O}_{31}$ (1207.14698, err. -0.794 ppm); ^1H and ^{13}C NMR (1% $\text{CDCl}_3/\text{DMSO}-d_6$): Tables 2 and 3.

3.6.2. Degalloyl-reduced rosacyanin A1 (6). Blue amorphous powder. UV–vis (0.1% HCl/MeOH) λ_{max} : 582 (log ϵ , 4.28), 360 (3.89), 260 (sh, 4.43) and 211 nm (4.70); HR-FT-ICR-MS: 903.12406 calculated for $\text{C}_{42}\text{H}_{31}\text{O}_{23}$ (903.12506, err. 1.116 ppm); ^1H and ^{13}C NMR [CD_3CN (CD_3CN): D_2O (H_2O):TFA- d (TFA)=50:50:0.5)]: Tables 2 and 3.

Supplementary data

Supplementary data associated with this article can be found in the online version, at doi:10.1016/j.tet.2006.07.068.

References and notes

- Goto, T. *Progress in the Chemistry of Organic Natural Products*; Herz, H., Griesbach, H., Kirby, G. W., Tamm, C., Eds.; Springer: Wien, New York, NY, 1987; Vol. 52, pp 113–158.
- Asen, S.; Stewart, R. N.; Norris, K. H. *Phytochemistry* **1972**, *11*, 1139–1144.
- Yabuya, T.; Nakamura, M.; Iwashina, T.; Yamaguchi, M.; Takehara, T. *Euphytica* **1997**, *98*, 163–167.
- Goto, T.; Kondo, T.; Tamura, H.; Imagawa, H.; Iino, A.; Takeda, K. *Tetrahedron Lett.* **1982**, *23*, 3695–3698.
- Lu, T. S.; Saito, N.; Yokoi, M.; Shigehara, A.; Honda, T. *Phytochemistry* **1992**, *31*, 659–663.
- Goto, T.; Kondo, T.; Tamura, H.; Kawahori, K.; Hattori, H. *Tetrahedron Lett.* **1983**, *24*, 2181–2184.
- Kondo, T.; Ueda, M.; Goto, T. *Tetrahedron* **1990**, *46*, 4749–4756.
- Goto, T.; Kondo, T.; Kawai, T.; Tamura, H. *Tetrahedron Lett.* **1984**, *25*, 6021–6024.
- Yoshida, K.; Kondo, T.; Okazaki, Y.; Katou, K. *Nature* **1995**, *373*, 291.
- Goto, T.; Tamura, H.; Kawai, T.; Hoshino, T.; Harada, N.; Kondo, T. *International Symposium on Bioorganic Chemistry*; Annals of the New York Academy of Sciences: New York, NY, 1986; Vol. 471, pp 155–173.
- Kondo, T.; Yoshida, K.; Nakagawa, A.; Kawai, T.; Tamura, H.; Goto, T. *Nature* **1992**, *358*, 515–518.
- Takeda, K.; Kariuda, M.; Itoi, H. *Phytochemistry* **1985**, *24*, 2251–2254.
- Figueiredo, P.; Elhabiri, M.; Toki, K.; Saito, N.; Dangles, O.; Brouillard, R. *Phytochemistry* **1996**, *41*, 301–308.
- Bloor, S. J.; Falshaw, R. *Phytochemistry* **2000**, *53*, 575–579.
- Fukui, Y.; Kusumi, T.; Yoshida, K.; Kondo, T.; Matsuda, C.; Nomoto, K. *Phytochemistry* **1998**, *47*, 1409–1416.
- Yoshida, K.; Toyama, Y.; Kameda, K.; Kondo, T. *Phytochemistry* **2000**, *54*, 85–92.
- Mol, J.; Cornish, E.; Mason, J.; Koes, R. *Curr. Opin. Biotechnol.* **1999**, *10*, 198–201.
- Eugster, C. H.; Fischer, E. M. *Angew. Chem., Int. Ed. Engl.* **1991**, *30*, 654–672.
- Tanaka, Y.; Fukui, Y.; Togami, J.; Katsumoto, Y.; Mizutani, M. WO Patent 2005/017147.
- Fukui, Y.; Kusumi, T.; Masuda, K.; Iwashita, T.; Nomoto, K. *Tetrahedron Lett.* **2002**, *43*, 2637–2639.
- Goto, T.; Kondo, T. *Angew. Chem., Int. Ed. Engl.* **1991**, *30*, 17–33.
- Yoshida, T.; Hatano, T.; Okuda, T. *Magn. Reson. Chem.* **1992**, *30*, S46–S55.
- Wilkins, C. K.; Bohm, B. A. *Phytochemistry* **1976**, *15*, 211–214.
- Yoshida, T.; Jin, Z. X.; Okuda, T. *Chem. Pharm. Bull.* **1991**, *39*, 49–54.
- Ma, Y. L.; Van den Heuvel, H.; Claeys, M. *Rapid Commun. Mass Spectrom.* **1999**, *13*, 1932–1942.
- Sinha, A.; Taylor, W. H.; Khan, I. H.; Mcdaniel, S. T.; Esko, J. D. *J. Nat. Prod.* **1999**, *62*, 1036–1038.
- Bakker, J.; Timberlake, C. F. *J. Agric. Food Chem.* **1997**, *45*, 35–43.
- Hatano, T.; Shida, S.; Han, L.; Okuda, T. *Chem. Pharm. Bull.* **1991**, *39*, 876–880.
- Nonaka, G.; Nishimura, H.; Nishioka, I. *J. Chem. Soc., Perkin Trans. 1* **1985**, 163–172.
- Nonaka, G.; Ishimaru, K.; Mihashi, K.; Iwase, Y.; Ageta, M.; Nishioka, I. *Chem. Pharm. Bull.* **1988**, *36*, 857–869.
- Okuda, T.; Yoshida, T.; Hatano, T.; Iwasaki, M.; Kubo, M.; Orime, T.; Yoshizaki, M.; Naruhashi, N. *Phytochemistry* **1992**, *31*, 3091–3096.
- Nayeshiro, K.; Eugster, C. H. *Helv. Chim. Acta* **1989**, *72*, 985–992.
- Mistry, V. T.; Cai, Y.; Lilley, H.; Haslam, E. *J. Chem. Soc., Perkin Trans. 2* **1991**, 1278–1296.
- Pfeffer, P. E.; Valentine, K. M.; Parrish, F. W. *J. Am. Chem. Soc.* **1979**, *101*, 1265–1274.